Journal of Atomic, Molecular, Condensate & Nano Physics
Vol. 7, No. 2, pp. 95–105, 2020
ISSN 2349-2716 (online); 2349-6088 (print)
Published by RGN Publications

http://www.rgnpublications.com

DOI: 10.26713/jamcnp.v7i2.1422

Research Article

The Effect of Manganese(Mn) Substitutional Doping on Structural, Electronic and Magnetic Properties of Pristine Hexagonal Graphene: Using Spin Polarized Density Functional Theory

Mitiku Yimer Anagaw and Sintayehu Mekonnen Hailemariam*

Department of Physics, College of Natural Sciences, Arba Minch University, Arba Minch, Ethiopia
***Corresponding author:** hailemariamsintayeh@email.com

Abstract. Graphene, a monolayer of carbon atoms packed in a hexagonal structure, has become one of the most remarkable materials available to condensed matter physics and material science(engineering) today due to its nobel structural and electronic properties. In this paper, the structural, electronic, and magnetic properties of Mn-doped monolayer pristine graphene is studied using spin-polarized *density functional theory* (DFT). The results show that the substitution of Mn dopant atom at the C sites is energetically favorable and the dopants are strongly hybridized with neighboring C-atoms of graphene. The *total density of state* (TDOS), *partial density of state* (PDOS), and energy band structure calculations results revel that the electronic and magnetic properties of pristine graphene is being affected in the presence of Mn dopants. Thus, in the presence of Mn dopants nonmagnetic(paramagnetic) and metallic state of pristine graphene is turned to half-metallic with the ferromagnetic ground state. Based on result, we recommend that Mn doped graphene is Nobel material for spintronics and magnetic information storage applications.

Keywords. Pristine graphene; Electronic structure; Density functional theory, Magnetic interaction

PACS. 31.10.+z; 31.15.E-; 71.10.-w; 71.15.Mb; 71.20.-b; 71.55.-i

Received: June 15, 2020 **Accepted:** July 10, 2020

1. Introduction

Graphene is a rapidly rising star on the horizon of materials science and condensed matter physics due to its remarkable properties, such as high thermal conductivity [1], electrical conductivity [2], extremely high tensile strength associated with strength of long carbon bonds [3]. All of aforementioned properties which giving it the potential for replacing commercial fillers currently in use for the fabrication of polymer composites and coatings. The carbon atoms of graphene are packed in the hexagonal pattern, often referred to as the honeycomb pattern [4]. There are two atoms (C) per unit cell. Each atom in the unit cell of the graphene layer has reflection symmetry. As both atoms in the unit cell are carbon atoms, there would be no physical difference if the graphene layer were to be replaced by its reflection, and also has rotational symmetry when it is rotated 120° an atom. Each atom has three nearest-neighbor atoms located at a distance of about 1.42 Å and shares a σ-bond with each of its three nearest neighbors, and has a fourth bond, called the π-bond, oriented out of the plane [5]. The entire graphene lattice can be described with the primitive cell containing the two carbon atoms A and B.

Pristine or pure graphene is nonmagnetic [6, 7] which deems(hinder) its application to spintronics and magnetic information storage. However, there is theoretical evidence that indicates that intrinsic properties of pure graphene can be modulated in the presence of transition metals like (Mn, Fe, Co, Ni etc.) [8–12] doping. On the other hand, *diluted magnetic semiconductors* (DMS) a new class of material that combines both the charge and spin of the electrons becomes a promising research area in material world. In today's technologies, two degrees of freedom of electrons: charge and spin can be well handled and applied to practical devices but separately [13]. The Combination of the charge and the spin of electrons will substantially increase the capabilities of electronics such as interesting technology that can be achieved by doping transition metal (Mn) [9]. The idea of doping graphene with manganese can allow graphene to be applied in the field of spintronics and advanced spintronics device applications [16]. But only a few study which focus on electronic structure [9] are studied on doped graphen recently. However, the detailed investigation of structural, electronic structure especially band structure, and magnetic properties of doped of graphene are not investigated in detail. In the current study structural properties; lattice parameters, bond length, and bond angle; electronic structure (total density of state (TDOS) and partial density of states (PDOS)), spin-polarized energy band structure were investigated for pure (pristine) and Mn-doped graphene where studied in detail. Furthermore, Mn-Mn distance-dependent magnetic properties of Mn-doped graphene were modeled using spin-polarized density functional theory.

2. Computional Details

First-principles calculations are performed based on spin-polarized DFT [17] using Quantum Espresso code [18]. *Ultrasoft pseudopotentials* (UPP) were used to deal with the interaction between valence electrons and the ionic core [19]. The plane-wave basis set with a cutoff energy

of 50 Ry was used after performing a convergence test. To investigate the doping effects of Mn impurities on pristine graphene, the graphene was modeled by the supercell of $(3 \times 3 \times 1)$ and $(4 \times 4 \times 1)$ containing 18 and 32 atoms. A large vacuum region of 15 Å was added to avoid interactions between adjacent layers along the z-axis. Integration over the *Brillouin zone* (BZ) was sampled based on Monkhorst pack 2D grid [20], which varies from $8 \times 8 \times 1$ and $16 \times 16 \times 1$ was used for structural relaxation and density of state calculation, respectively. Structural optimizations were performed for all configurations using the conjugate gradient algorithm until each component of the interatomic force became less than 0.027 eV/Å. After structural optimizations doping were managed by replacing one (two) atoms from graphene with manganese (Mn).

3. Effect of Single Manganese Doping on Structural Properties of Pristine Graphene

3.1 Bond length,bond angle and lattice constant for pristine and single Mn doped graphene

First, a geometry optimization was performed for the pristine graphene sheet, allowing all C atoms to relax. As shown in Table 1 the C−C bond lengths of pure optimized graphene were found to be 1.4203 Å which is closer to other recently reported results [23]. However, after the substitution of single Mn, the C−C bond length around dopant atom measured to be 1.3720 Å and 1.3800 Å for $3 \times 3 \times 1$ and $4 \times 4 \times 1$ supercell, respectively. In addition to this, as a result of Mn doping the adjoining C−Mn bond lengths are increased to 1.6451 Å and 1.6606 Å, for the detail see Table 1. After structural optimization, the equilibrium lattice constant of pristine graphene was found to be 2.8495 Å, but after substitution of single Mn in C-cite the calculated lattice constants was measured to be 2.8760 Å for $4 \times 4 \times 1$ supercells as shown in Table 1. This extension in lattice constant and bond lengths results in a decrease of C−C bond lengths in the proximity of the Mn-dopant. This might be due to a larger atomic radius of Mn (1.7900 Å) atom as compared to C (0.9100 Å) atom.

However, as shown in Table 1 and Figure 1, substitution of Mn atom does not destroy the planarity of graphene sheet and the structural deformation are much localized around the doping site.

Table 1. The calculated lattice constant, bond length and bond angle for pure and Mn doped graphene

Supercells	System	C−C bond length (Å)	C_1-Mn_1 bond length (Å)	C_2-Mn_1 Bond length (Å)	Lattice constant (Å)	Bond angle (°)
$3 \times 3 \times 1$	pure	1.420	-	-	2.460	120
	1Mn doped	1.372	1.645	1.645	2.8495	112.513
$4 \times 4 \times 1$	pure	1.420	-	-	2.460	120
	1Mn doped	1.380	1.660	1.66	2.876	112.981

The calculated bond angle (C−C−C) for pristine graphene was found to be 120° as shown in Table 1 after substitution of single Mn atom the bond angle (C−Mn−C) found to be 112.213° and 112.981° respectively for $3\times3\times1$ and $4\times4\times1$ suppecells. However, in agreement with reference [25] the introduction of Mn atoms do not show any out-of-plane displacement.

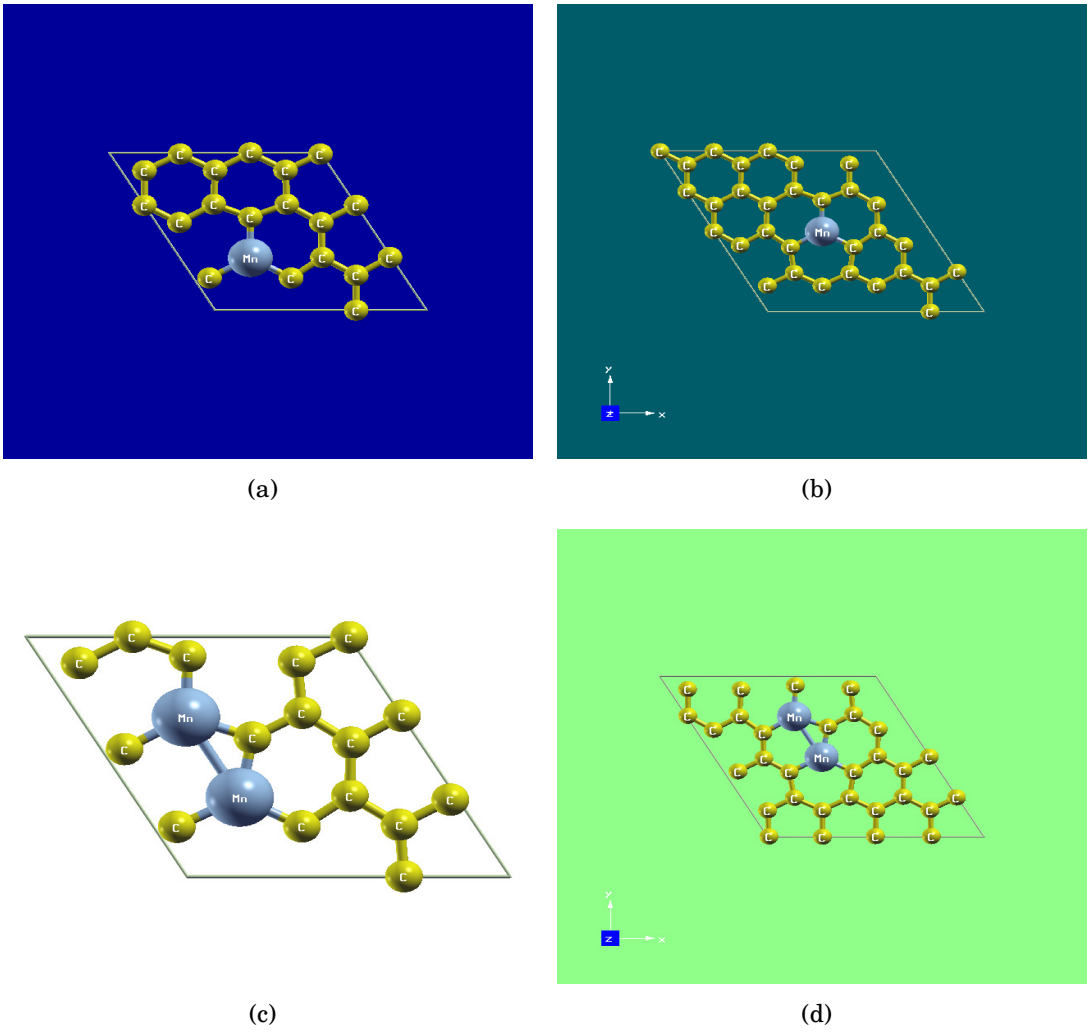

Figure 1. Relaxed input structure of $3\times3\times1$ and $4\times4\times1$ graphene super-cells: (a) and (b) pure, (c) and (d) single manganese doped, and (e) and (f) two manganes doped graphene

3.2 Defect formation energy and structural stability

To understand relative stability of dopant atom (Mn) in graphene (C), the dopant formation energy (E_{form}) were carried out using the following formula [14, 15]:

$$E_{form} = E_{tot}(Mn,C) - E_{tot}(C) - \sum_i n_i(\mu_{Mn} - \mu_C), \tag{3.1}$$

where $E_{tot}(Mn,C)$ and $E_{tot}(C)$ are total energies of doped and pure graphene (C) respectively, n_i is the corresponding number of species that have been added to or removed from the super cell and μ_C and μ_{Mn} are chemical potentials of Mn and C respectively.

Table 2. The calculated defect formation energy of Mn-doped graphene for different suppercells

System	E_{Tot} (eV)	E_c (eV)	μ_{Mn} (eV)	μ_C (eV)	E_{form} (eV)
1Mn doped 3×3	−5522.25610	−2814.12242	−2862.24286	−156.29940	−2.19022
2Mn doped 3×3	−8230.55931	−2814.12242	−2862.24286	−156.29940	−4.54997
2Mn doped 4×4	−10420.33231	−5002.77054	−2862.24286	−156.29940	−5.67485

Here the chemical potential for Mn (μ_{Mn}) is obtained from its bulk BCC Mn, and the chemical potential of graphene (μ_C) is also obtained from a the most stable form of carbon called graphite. The calculated results are summarized in Table 2. As can be seen from Table 2, the calculated defect formation energies (E_{form}) of various Mn-doped configuration are which confirm that Mn-doped graphene supercell is structurally stable and the dopants are strongly bonded with neighboring C-atoms.

4. Effect of Single Manganese (Mn) Doping on Electrical Properties of Pristine Graphene

4.1 Total spin polarized Density of state fore pristine and manganese doped graphene

By analyzing the total spin polarized density of states (TDOS) in pristine and Mn-doped graphene it is observed that on substituting C atom with Mn atom the TDOS gets altered and localized levels start to appear, especially in the vicinity of Fermi-level (E_F) as shown in Figure 2. Moreover, as impurity concentration increase from 3.125% to 11.11% the impurity state in the vicinity of Fermi level broaden in width for the detail see Figure 2(a-e) which open the room to control the electronic and magnetic properties of those materials by manipulating the concentration of dopants (Mn) which is platform to use graphene as dilute magnetic semiconductor for spintronics application.

4.2 Partial density of states for pristine and doped graphene

To explore the contribution of various states in total DOS, the *partial density of state* (PDOS) is investigated for pristine and doped graphene. PDOS graph from Figure 3 is showing that near the Fermi level the main contribution is derived from p-orbital electrons of carbon and hence these electrons are expected to participate in conduction processes. Figure 3(c) shows that after doping the contribution of 2p states transpires still maximum near the Fermi level. However, the majority of the contribution state in the vicinity of Fermi-level for Mn-doped graphene is derived from Mn 3d orbitals These states are responsible for generating localized magnetism and metallic character. On the other hand, the contribution of $C(S)$ state towards total PDOS is almost zero which justifies the $C(S)$ electrons remain isolated and are not responsible for any bonding.

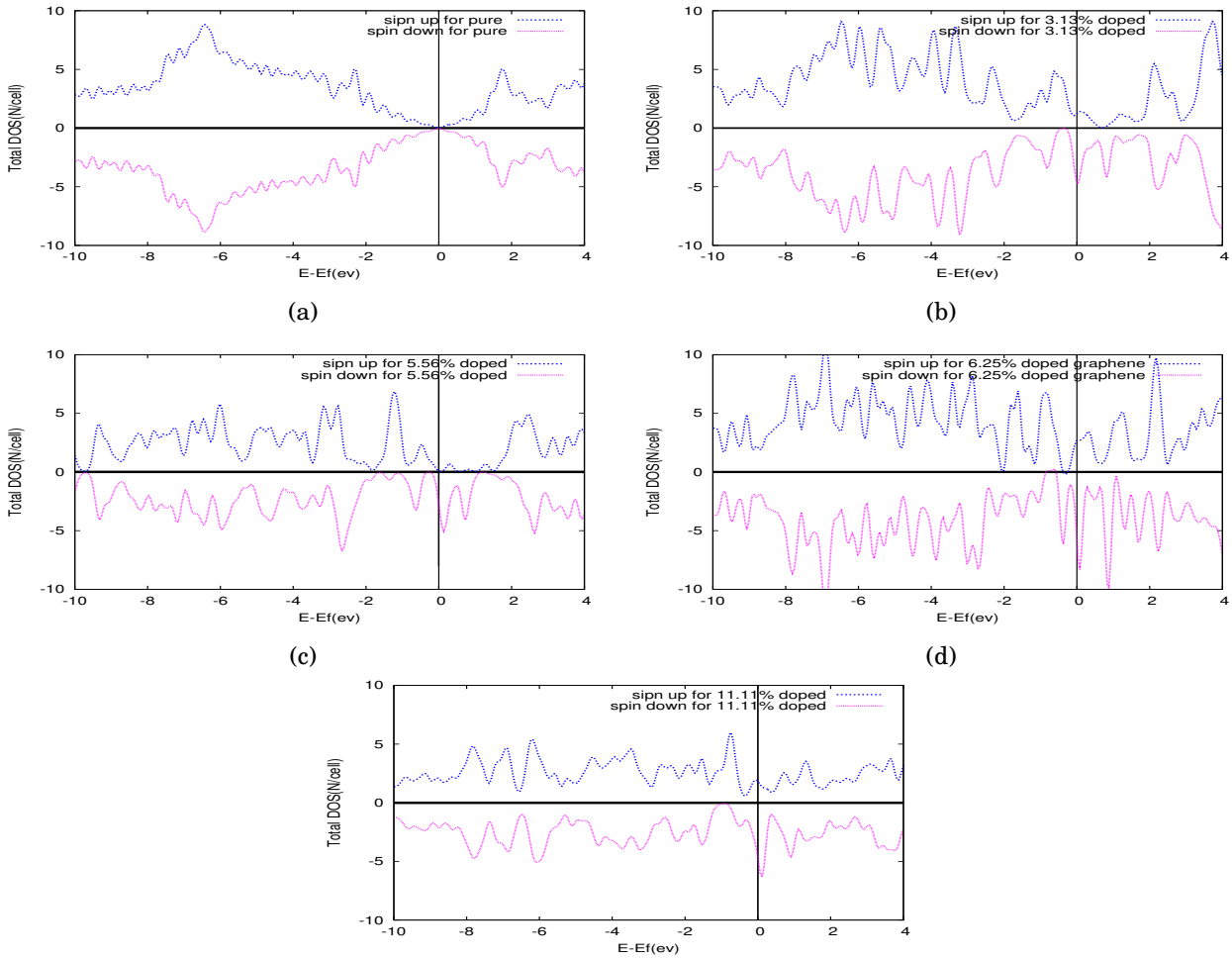

Figure 2. The calculated DOS for: (a) pure graphene, (b) 3.13% Mn doped graphene, (c) 5.56% Mn doped graphene, (d) 6.25% Mn doped graphene, and (e) 11.11% Mn doped graphene. The zero energy represent Fermi level, the blue and purple lines represents spin-up and spin-down, respectively

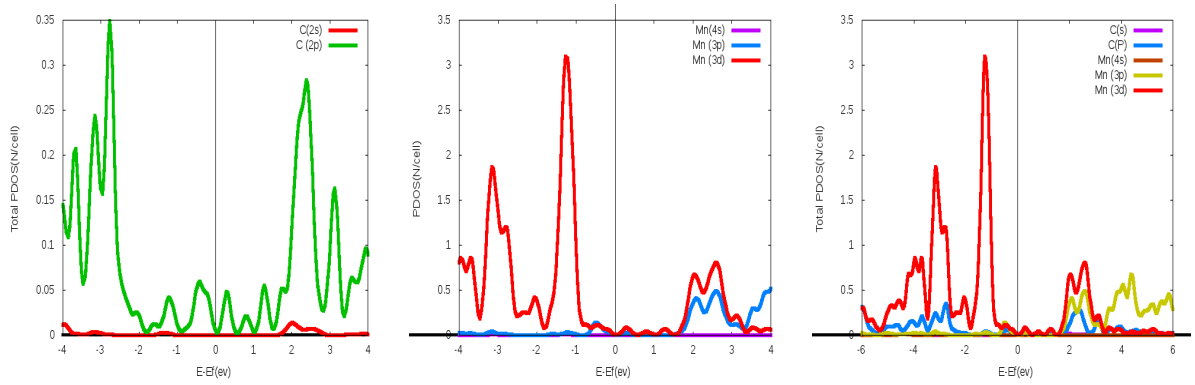

Figure 3. The calculated Partial density of states (PDOS) for pristine and Mn doped graphene carbon ($C_{s,p}$) orbital (a), manganese (Mn-$_{s,p,d}$) orbital (b) and carbon and manganese (C-$_{s,p}$) and (Mn-$_{s,p,d}$) orbital (c)

4.3 Band structure of pure and doped graphene

To investigate the effect of Mn-doping on electronic energy band structure, the band stricture of pristine and single Mn-doped graphene was plotted by following Γ-K-M-Γ path of 2D hexagonal Brillouin zone (Bz) of graphene. As shown in Figure 4(a,b) the band structure of pure graphene shows that the minimum of the conduction band and the maximum of the valence band are intersecting at the K point. This means that the electrons and holes behave as massless Dirac Fermions [28] and they can move with the speed of 300 times less than the speed of light [2], and hence pristine graphene becomes a zero-gap material. This result is in good agreement with other reports [29]. As shown from Figure 4(c,d) in the case of single Mn-doped graphene, the conduction band minimum and valence band maximum points are shifted and a small opening of bandgap especially on the energy band structure of spin upstate is observed see Figure 4(c). Therefore, the spin symmetry is broadened in the presence of Mn dopants which confirms the inducement of ferromagnetic ordering in Mn-doped graphene as discussed the next section.

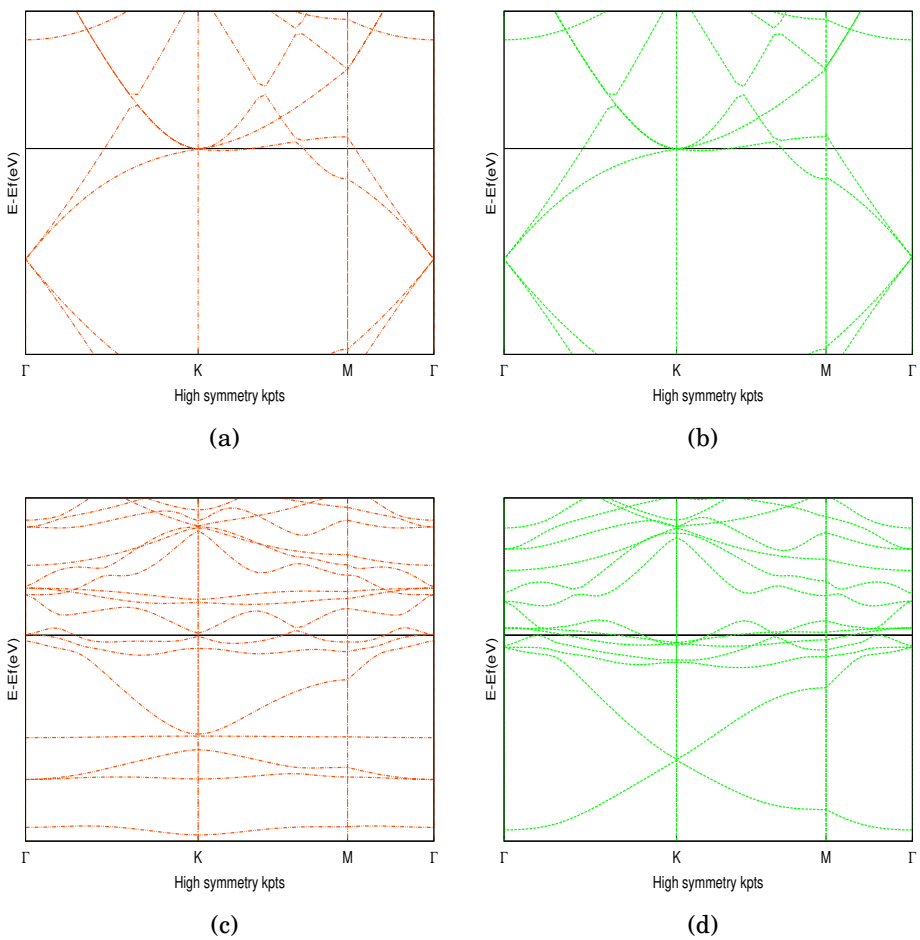

Figure 4. The calculated band structure for graphene; (a) pristine spin up, (b) pristine spin down, (c) spin up for single Mn-doped graphene and (d) spin down for single Mn-doped graphene. The zero-energy represent Fermi level, the blue and green lines represent spin-up and spin-down respectively

5. Effect of Manganese Doping on Magnetic Properties of Pristine Graphene

From spin polarized DFT calculation the magnetic moment of pure graphene supper cell of $3 \times 3 \times 1$ and $4 \times 4 \times 1$ were found to be 0 μ_B. However, after introducing single manganese (Mn) in aforementioned super cell, the magnetic moments are measured to be 2.61 μ_B and 1.90 μ_B respectively and hence the system becomes ferromagnetic see Table 3. Thus,the ferromagnetic property most likely originates from asymmetric spin states (DOS around the Fermi level).

Table 3. The calculated total energy in Ferromagnetic state (E_{FM}), total Antiferromagnetic state (E_{AFM}), and the energy difference ($\Delta(E)$) and total magnetic moment per supercell (μ) of Mn doped graphene

Supercell	E_{FM} (Ry)	E_{AFM} (Ry)	ΔE (Ry)	$\mu(\mu_B)$	magnetic ground state
$3 \times 3 \times 1$ pristine	-	-	-	0.00	Paramagnetic
$3 \times 3 \times 1$ 1Mn doped		-	-	2.61	Ferromagnetic
$3 \times 3 \times 1$ 2Mn doped	−604.93473212	−604.94383237	0.00910025	2.96	Antiferromagnetic
$4 \times 4 \times 1$ pristine	-	-	-	0.00	Paramagnetic
$4 \times 4 \times 1$ 1Mn doped	-	-	-	1.90	Ferromagnetic
$4 \times 4 \times 1$2Mn doped	−765.88002036	−765.89230931	0.01228895	2.60	Antiferromagnetic

On the best of our theoretical understanding, the magnetic properties of Mn-doped graphene can be explained in terms of the hybridization between C(2p) orbital and Mn(3d) orbits. Thus, the neighboring C 2p orbitals strongly interact with the Mn atom ($3d^5$ orbital electrons) and which further indicates with other C(2p) orbitals. Therefore, the presence p-d magnetic exchange mechanism which stabilizes ferromagnetic ground state in doped graphene.

5.1 Magnetic interaction between dopants

In a doped system like Mn-doped graphene as the number of dopants exceed to single, how dopant that magnetic impurity interact with each other and stabilizes the magnetic ground state is another difficult issue in the field of magnetic semiconductors. To address such issue the magnetic energy (ΔE), the energy difference between the two dopants are in *ferromagnetic* (FM) configuration and *Antiferromagnetic* (AFM) configuration were evaluated using the following relation [26, 27]

$$\Delta E = E_{FM} - E_{AFM}. \tag{5.1}$$

As shown from Table 3 the calculated magnetic energy was +0.00910025 and +0.01228895 Ry respectively for supercells of 3×3, and 4×4. Therefore, two dopants located at the nearest neighbor distance (NN=2.460 Å) are favored to interact Antiferromagnetically to stabilize their magnetic ground state.

6. Conclusion

The structural, electronic, and magnetic properties of Mn-doped pristine graphene was studied using spin-polarized DFT. The calculated results indicate that the substitution of Mn in pristine graphene affects its structural properties: the bond length, bond angle and lattice parameters increase due to the large atomic size of Mn in comparison to C-atom of graphene. In addition to this, the calculated defect formation energy confirms that Mn-doped graphene is energetically stable and the dopants are strongly hybridized with nearest neighboring C-atoms. Besides to this, it is also found that the substitution of single Mn atom (doping) in graphene supercell turns the nonmagnetic semiconductor properties of the pure system to half-metallic and ferromagnetic. Furthermore, the findings also confirm that two dopants located at the nearest neighbor distance are favored to interact Antiferromagnetically to stabilize their magnetic ground state. Based on our result we suggest that Mn doped-graphene are a good candidate in the diluted magnetic semiconductors for spintronics application and magnetic information storage if the detailed experimental investigation is made.

Data Availability

The data used to support the findings of this study are available from the corresponding author upon request.

Acknowledgements

We acknowledge financial support of Amhara educational office and Ethiopian Ministry of eduction for financial support and Arbaminch University, Arbaminch, Ethiopia for providing the computational facilities.

Competing Interests

The authors declare that they have no competing interests.

Authors' Contributions

All the authors contributed significantly in writing this article. The authors read and approved the final manuscript.

References

[1] H. Malekpour, K.-H. Chang, J.-C. Chen, C.-Y. Lu, D. L. Nika, K. S. Novoselov and A. A. Balandin, Thermal conductivity of graphene laminate, *Nano Letters* **14** (9) (2014), 5155 – 5161, DOI: 10.1021/nl501996v.

[2] S. Morozov, K. Novoselov, M. Katsnelson, F. Schedin, D. Elias and J. Jaszczak, Giant. intrinsic carrier mobilities in graphene and its bilayer, *Physical Review Letter* **100**(1) (2008), 016602, DOI: 10.1103/PhysRevLett.100.016602.

[3] C. Lee, X. Wei, J. W. Kysar and J. Hone, Measurement of the elastic properties and intrinsic strength of monolayer graphene, *Science* **321** (5887) (2008), 385 – 388, DOI: 10.1126/science.1157996.

[4] M. J. Allen, V. C. Tung and R. B. Kaner, Honeycomb carbon: a review of graphene, *Chemical Reviews* **110** (2010), 132 – 145, DOI: 10.1021/cr900070d.

[5] A. Kekulé, *Bulletin de la Societe Chimique de Paris* **3**(2) (1865), 98, `https://gallica.bnf.fr/ark:/12148/bpt6k281952v/f102.image`; Untersuchungen über aromatische Verbindungen Ueber die Constitution der aromatischen Verbindungen. I. Ueber die Constitution der aromatischen Verbindungen, *Annalen der Chemie und Pharmazie* **137**(2) (1866), 129, DOI: 10.1002/jlac.18661370202.

[6] M. Sepioni, R. R. Nair, S. Rablen, J. Narayanan, F. Tuna, R. Winpenny, A. K. Geim and I. V. Grigorieva, Limits on intrinsic magnetism in graphene, *Physical Review Letter* **105** (2010), 207205, DOI: 10.1103/PhysRevLett.105.207205

[7] R. J. Toh, H. L. Poh, Z. Sofer and M. Pumera, Transition metal (Mn, Fe, Co, Ni)-doped graphene hybrids for electrocatalysis, *Chemistry an Asian Journal* **8** (2013), 1295 – 1300, DOI: 10.1002/asia.201300068.

[8] T. Hou, L. Kong, X. Guo, Y. Wu, F. Wang, Y. Wen and H. Yang, Magnetic ferrous-doped graphene for improving Cr(VI) removal, *Materials Research Express* **3**(4) (2016), 045006, DOI: 10.1088/2053-1591/3/4/045006.

[9] M. Wu, C. Cao and J. Z. Jiang, Electronic structure of substitutionally Mn-doped graphene, *New Journal of Physics* **12** (2010), 063020, DOI: 10.1088/1367-2630/12/6/063020.

[10] G. Bertoni, L. Calmels, A. Altibelli and V. Serin, First-principles calculation of the electronic structure and eels spectra at the graphene/Ni(111) interface, *Physical Review B* **71**(7) (2005), 075402, DOI: 10.1103/PhysRevB.71.075402.

[11] V. M. Karpan, G. Giovannetti, P. A. Khomyakov, M. Talanana, A. A. Starikov, M. Zwierzycki, J. van den Brink, G. Brocks and P. J. Kelly, Graphite and graphene as perfect spin filters, *Physical Review Letter* **99**(17) (2007), 1766021, DOI: 10.1103/PhysRevLett.99.176602.

[12] V. M. Karpan, P. A. Khomyakov, A. A. Starikov, G. Giovannetti, M. Zwierzycki, M. Talanana, G. Brocks, J. van den Brink and P. J. Kelly, Theoretical prediction of perfect spin filtering at interfaces between close-packed surfaces of Ni or Co and graphite or graphene, *Physical Review B* **78**(19) (2008), 195419, DOI: 10.1103/PhysRevB.78.195419.

[13] M. Noga, Separation of charge and spin degrees of freedom in the Hubbard model, *Czechoslovak Journal of Physics* **42** (1992), 823 – 841, DOI: 10.1007/BF01904154.

[14] R. Mishra, W. Zhou, S.J. Pennycook, S. T. Pantelides and J.-C. Idrobo, Long-range ferromagnetic ordering in manganese-doped two-dimensional dichalcogenides, *Physical Review B* **88** (2013), 144409, DOI: 10.1103/PhysRevB.88.144409.

[15] K. F. Mak, C. Lee, J. Hone, J. Shan and T. F. Heinz, Atomically thin MoS_2: a new direct-gap semiconductor, *Physical Review Letter* **105** (2010), 136805, DOI: 10.1103/PhysRevLett.105.136805 .

[16] M. L. Ould Ne, A. Abbassi, A. G. El hachimi, A. Benyoussef, H. Ez-Zahraouy and A. El Kenz, Electronic, optical, properties and widening band gap of graphene with Ge doping, *Optical and Quantum Electronics* **49** (2017), Article number 218, DOI: 10.1007/s11082-017-1024-5.

[17] A. Kheyri, Z. Nourbakhsh and E. Darabi, Effect of Fe, Co, Si and Ge impurities on optical properties of graphene sheet, *Thin Solid Films* **612** (2016), 214 – 224, DOI: 10.1016/j.tsf.2016.06.007

[18] P. Giannozzi, S. Baroni, N. Bonini, M. Calandra, R. Car, C. Cavazzoni, D. Ceresoli, G. L. Chiarotti, M. Cococcioni, I. Dabo, A. D. Corso, S. de Gironcoli, S. Fabris, G. Fratesi, R. Gebauer, U. Gerstmann, C. Gougoussis, A. Kokalj, M. Lazzeri, L. Martin-Samos, N. Marzari, F. Mauri, R. Mazzarello, S. Paolini, A. Pasquarello, L. Paulatto, C. Sbraccia, S. Scandolo, G. Sclauzero, A. P. Seitsonen, A. Smogunov, P. Umari and R. M. Wentzcovitch, QUANTUM ESPRESSO: a modular and open-source software project for quantum simulations of materials, *Journal of Physics: Condensed Matter* **21** (2009), 395502, DOI: 10.1088/0953-8984/21/39/395502.

[19] N. Troullier and J. L. Martins, Efficient pseudopotentials for plane-wave calculations, *Physical Review B* **43** (1993), 1993 – 2006, DOI: 10.1103/PhysRevB.43.1993.

[20] H. J. Monkhorst and J. D. Pack, Special points for Brillouin-zone integrations, *Physical Review B* **B13** (1976), 5188 – 5192, DOI: 10.1103/PhysRevB.13.5188

[21] L. Hu, Y. Sun, Y. Zhou, L. Bai, Y. Zhang, M. Han, H. Mumei, L. Hui, Y. Liu, and Z. Kang, Nitrogen and sulfur co-doped chiral carbon quantum dots with independent photoluminescence and chirality, *Inorganic Chemistry Frontiers* **4**(6) (2017), 946 – 953, DOI: 10.1039/C7QI00118E

[22] J. M. Carlsson and M. Scheffler, Structural, electronic and chemical properties of nanoporous carbon, *Physical Review Letters* **96** (2006), 046806, DOI: 10.1103/PhysRevLett.96.046806.

[23] O. Olaniyan, R. E. Mapasha, D. Y. Momodu, M. J. Madito (Moshawe), A. A. Kahleed, F. U. Ugbo, A. Bello, F. Barzegar, K. O. Oyedotun, N. I. Manyala, Exploring the stability and electronic structure of beryllium and sulphur Co-doped graphene: first principles study, *RSC Advances* **6** (2016), 88392 – 88402, `http://hdl.handle.net/2263/60303`.

[24] S. Ullah, A. Hussain, W. A. Syed, M. A. Saqlain, I. Ahmad, O. Leenaertse and A. Karimf, Band-gap tuning of graphene by Be doping and Be, B co-doping: a DFT study, *RSC Advances*, **5**(69) (2015), 55762 – 55773, DOI: 10.1039/C5RA08061D.

[25] D. Usachov, O. Vilkov, A. Grüneis, D. Haberer, A. Fedorov, V. K. Adamchuk, A. B. Preobrajenski, P. Dudin, A. Barinov, M. Oehzelt, C. Laubschat and D. V. Vyalikh, Nitrogen-doped graphene: efficient growth, structure, and electronic properties, *Nano Letters* **11**(12) (2011), 5401 – 5407, DOI: 10.1021/nl2031037.

[26] S. Mekonnen and P. Singh, Electronic structure and nearly room-temperature ferromagnetism in V-doped monolayer and bilayer MoS_2, *International Journal of Modern Physics B* **32**(21) (2018), 1850231, DOI: 10.1142/S0217979218502314.

[27] S. M. Hailemariam, Electronic structure and room temperature of 2D dilute magnetic semiconductors in bilayer MoS_2 doped Mn, *Advances in Condensed Matter Physics* **2020** (2020), Article ID 9635917, 8 page, DOI: 10.1155/2020/9635917.

[28] K. S. Novoselov, A. K. Geim, S. V. Morozov, D. Jiang, M. I. Katsnelson, I. V. Grigorieva, S. V. Dubonos and A. A. Firsov, Two-dimensional gas of massless Dirac fermions in graphene, *Nature* **438** (2005), 197, DOI: 10.1038/nature04233.

[29] A. H. C. Neto, F. Guinea, N. M. R. Peres, K. S. Novoselov and A. K. Geim, The electronicproperties of graphene, *Reviews of Modern Physics* **81** (2009), 109, DOI: 10.1103/RevModPhys.81.109.